

RECEIVED

OCT 24 1997

OSTI

The Argonne Laser-Driven D Target: Recent Developments and Progress.

J. A. Fedchak, K. Bailey, W. J. Cummings, H. Gao,
C. E. Jones¹, R. S. Kowalczyk, J. Magnes², and M. Pipes³

Argonne National Laboratory
Argonne, IL 60439-4843

ANL/PHY/CP-94607
CONF-970894

Abstract.

The first direct measurements of nuclear tensor polarization p_{zz} in a laser-driven polarized D target have been performed at Argonne. We present p_{zz} and electron polarization P_e data taken at a magnetic field of 600 G in the optical pumping cell. These results are highly indicative that spin-temperature equilibrium is achieved in the system. To prevent spin relaxation of D and K atoms as well as the molecular recombination of D atoms, the walls of the laser-driven D target are coated with organosilane compounds. We discuss a new coating technique, the "afterwash", developed at Argonne which has yielded stable atomic fraction results when the coating is exposed to K. We also present new coating techniques for glass and Cu substrates.

I INTRODUCTION

Preliminary results of the first direct measurement of nuclear polarization in a laser-driven D target were reported nearly two years ago by Fedchak, Jones, and Kowalczyk [1]. Since then, the Argonne group has performed a systematic study of the nuclear tensor polarization p_{zz} and has developed a new coating technique, the "afterwash". A laser-driven H and D internal target has been installed in the Cooler ring at IUCF by the CE66/68 collaboration, representing the first use of a laser-driven H and D target in a nuclear physics experiment [2]. Here we will summarize the afterwash coating technique and also present new coating techniques for Cu and glass substrates which are currently being developed at Argonne. Additionally, we will present results of nuclear tensor polarization measurements in a laser-driven target with $B = 600$ G

- 1) Present address: Kellogg Lab 106-38, Caltech, Pasadena, CA 91125
- 2) Dept. of Physics, U. of Delaware
- 3) Dept. of Industrial Technology, Western Illinois U.

MASTER

DISTRIBUTION OF THIS DOCUMENT IS UNLIMITED 

The submitted manuscript has been authored by a contractor of the U. S. Government under contract No. W-31-109-ENG-38. Accordingly, the U. S. Government retains a nonexclusive, royalty-free license to publish or reproduce the published form of this contribution, or allow others to do so, for U. S. Government purposes.

DISCLAIMER

This report was prepared as an account of work sponsored by an agency of the United States Government. Neither the United States Government nor any agency thereof, nor any of their employees, make any warranty, express or implied, or assumes any legal liability or responsibility for the accuracy, completeness, or usefulness of any information, apparatus, product, or process disclosed, or represents that its use would not infringe privately owned rights. Reference herein to any specific commercial product, process, or service by trade name, trademark, manufacturer, or otherwise does not necessarily constitute or imply its endorsement, recommendation, or favoring by the United States Government or any agency thereof. The views and opinions of authors expressed herein do not necessarily state or reflect those of the United States Government or any agency thereof.

DISCLAIMER

**Portions of this document may be illegible
in electronic image products. Images are
produced from the best available original
document.**

in the optical pumping cell. A detailed report of the p_{zz} measurements is forthcoming [3].

II PHYSICS OF THE LASER-DRIVEN TARGET

In the laser-driven D target, K atoms are polarized by optical pumping with polarized laser light in a high magnetic field. The electron polarization is transferred to D atoms in D-K spin-exchange collisions. Deuterium electron polarization is subsequently transferred to the deuterium nucleus in D-D spin-exchange collisions. Walker and Anderson [4] have examined the consequences of D-D spin-exchange collisions in a laser-driven polarized D target. In the limit of many spin-exchange collisions, the population distribution of the six magnetic ground substates of deuterium will come to an equilibrium distribution characteristic of the total angular momentum pumped into the system by the laser. At equilibrium, the relative population of a given deuterium magnetic substate is given by

$$n(m_I) = e^{\beta m_I}, \quad (1)$$

where β^{-1} is a parameter known as the spin-temperature and m_I is the projection of the nuclear spin on the spin quantization axis. Eq. (1) can be used to calculate both the p_{zz} and the electron polarization P_e at equilibrium. The timescale for attaining spin-temperature equilibrium is inversely proportional to the D density n_D , and sets the timescale for polarizing the nucleus. Spin-temperature equilibrium in a laser-driven target has been discussed in several previous publications [1,5-7].

III EXPERIMENTAL APPARATUS

A schematic of the laser-driven target is shown in Fig. 1. Details of the experiment can be found in Refs. [3,5,6] and will only be summarized here. Deuterium flows into a rf discharge which dissociates the molecular deuterium into atoms. Deuterium atoms and molecules flow from the dissociator into a cylindrical optical pumping cell which lies between two pole faces of an electromagnet. The optical pumping cell has a diameter of 2.2 cm and a length of 4.6 cm. Potassium enters the cell through a 0.9 mm aperture connected to a K reservoir heated to 180°C, corresponding to a K density of $3.8 \pm 0.8 \times 10^{11} \text{ cm}^{-3}$. The $4^2S_{1/2} - 4^2P_{1/2}$ resonance of K is optically pumped by about 2 W of circularly polarized light from a Ti:sapphire ring laser broadened by an electro-optical modulator to match the Doppler width of the σ_+ or σ_- transition. Atoms experience about 700 wall bounces in the optical pumping cell and enter the transport tube through a 3.1 mm aperture. The pumping cell and Pyrex transport tube are heated to between 200°C and 250°C to

LASER-DRIVEN \vec{D} TARGET AND POLARIMETER

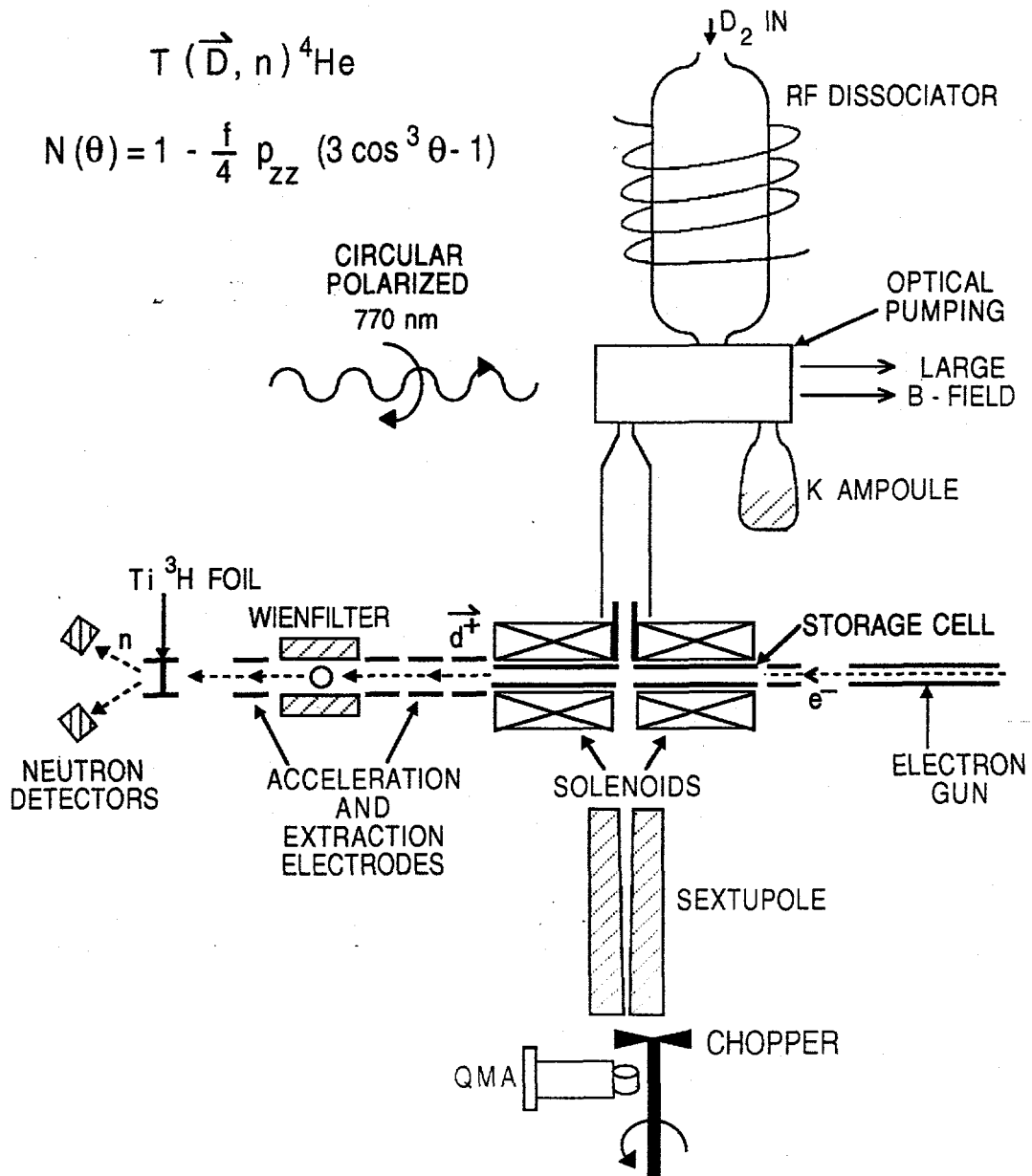


FIGURE 1. Schematic of the laser-driven D target.

prevent K from condensing on the walls. The Pyrex transport tube extends to a length of 30 cm, has a diameter of 19 mm, and is joined to a 6 cm length of aluminum tube by a viton O-ring. Atoms exiting the extended transport tube flow into an open ended aluminum storage cell 48 cm in length and 23 mm in diameter. Both the storage cell and aluminum section of the transport tube are heated to over 200°C. A 5 mm hole in the center of the storage cell allows the P_e polarimeter to sample atoms leaving the transport tube.

The P_e polarimeter is located downstream of the transport tube and has an acceptance such that the polarimeter samples atoms which have made many wall collisions in the transport tube. A sextupole magnet focuses atoms with spin up and defocuses those with spin down. Focused atoms pass through a chopper wheel and are detected by a quadrupole mass analyzer (QMA). A removable shutter placed before the sextupole allows one to measure the background signal in the QMA. Atomic polarization can be measured by blocking and unblocking the laser beam. The atomic polarization is determined by:

$$P_e = \frac{n_{\uparrow} - n_{\downarrow}}{n_{\uparrow} + n_{\downarrow}} = \frac{n_{unblocked}}{n_{blocked}} - 1, \quad (2)$$

where $n_{\uparrow(\downarrow)}$ denotes deuterium atomic states with electron spin up (down) and $n_{(un)blocked}$ is the signal measured with the QMA with the laser beam (un)blocked.

The atomic fraction, f_a , defined as the total number of deuterium nuclei in the form of atoms over the total number of deuterium nuclei (in the form of D or D₂) is also determined using the P_e polarimeter. This is determined with the QMA by measuring the mass 4 (amu) signal with the dissociator rf power on and off:

$$f_a = 1 - \frac{n_{on}}{n_{off}}. \quad (3)$$

With the rf power off the mass 4 signal n_{off} is entirely due to D₂, but when the dissociator rf power is turned on the mass 4 signal, n_{on} , measures the molecular flow from D₂ molecules that are not dissociated before entering the optical pumping cell and from D atoms which recombine on surfaces between the time they leave the dissociator and when they reach the QMA. For both f_a and P_e , the error in the measurements are dominated by systematic uncertainties and is less than 2%.

In addition to P_e , we can also measure the nuclear tensor polarization p_{zz} , defined by

$$p_{zz} = 1 - 3n_0, \quad (4)$$

where n_0 represents the fractional population density of the nuclear spin sub-states with $m_I = 0$. The p_{zz} polarimeter is based upon the technique developed by Price and Haeberli [8]. To determine p_{zz} the polarimeter employs the low

energy ${}^2\text{H} + {}^3\text{H} \rightarrow \text{n} + {}^4\text{He}$ reaction in which the angular distribution of the outgoing neutrons is anisotropic if the incident deuterium ions are tensor polarized. The expression for the differential cross section for a tensor polarized incident deuteron beam is

$$\sigma(\theta) = \sigma_0(\theta) \left(1 - \frac{f}{4} p_{zz} (3 \cos^2 \theta - 1) \right), \quad (5)$$

where σ_0 is the unpolarized cross section, which is isotropic in the center-of-mass frame, θ is the angle between the direction of the outgoing neutron and the spin of the deuteron in the center-of-mass system, and the dilution factor f accounts for the small admixture of reaction channels which have no tensor analyzing power. For ion energies in the range used for the polarimeter, the dilution factor has been measured and found to be near unity ($f \approx 0.96$) [9]. The neutron anisotropy R , defined as

$$R = \frac{\sigma(0^\circ)}{\sigma(90^\circ)} = \frac{1 - \frac{f}{2} p_{zz}}{1 + \frac{f}{4} p_{zz}}, \quad (6)$$

is measured with and without the optical pumping light incident on the pumping cell. The ratio of the measured R values for polarized and unpolarized ions is used to determine the tensor polarization of the deuterons in the storage cell. Differences in the detector efficiencies and angular acceptance largely cancel in the ratio.

A 2 keV electron beam directed along the length of the storage cell ionizes the deuterium atoms to produce D^+ . A solenoidal coil surrounding the storage cell creates the magnetic holding field of about 300 G that serves both to separate the deuterium magnetic substates and act as a guide field for the ions to prevent them from hitting the cell walls. Ions are extracted from the storage cell and accelerated towards a tritiated foil target mounted inside an electrostatic lens maintained at a potential of 50 kV. A Wien filter ($\vec{E} \times \vec{B}$) located between the storage cell and tritiated foil acts as a velocity selector to separate deuterium atoms and molecules. The deuteron spin direction, which is parallel to the solenoidal holding field in the storage cell, precesses by 45° in the B -field of the Wien filter. Neutrons resulting from the fusion reaction ${}^3\text{H}(d, n)\alpha$ are detected in two NE110 scintillators placed parallel and perpendicular to the spin direction, thus maximizing the neutron anisotropy in the two detectors.

Tests of the polarimeter with unpolarized deuterium show that the measurements are reproducible to better than $\Delta R/R = 0.01$. Corrections for the variation of p_{zz} due to the angular acceptance contribute an uncertainty of $\Delta p_{zz}/p_{zz} < 0.005$. The overall systematic error is dominated by the uncertainty in the spin rotation angle in the Wien filter, which gives a contribution of $\Delta p_{zz}/p_{zz} < 0.065$.

IV COATING TECHNIQUES AND TESTS

In order to reduce the recombination on surfaces as well as preserve D and K polarization, the Pyrex glassware is coated using SC-77 plus a trimethylmethoxysilane "afterwash", while the aluminum storage cell and short connecting tube are coated with a mixture of dimethyldimethoxysilane and methyltrimethoxysilane. Both the afterwash technique and aluminum coating techniques are discussed in ref. [10]. Below we will summarize the afterwash technique developed at Argonne, and present measurements relevant to the Pyrex glassware used during the p_{zz} measurements. We will also present new developments in the technique of coating Cu surfaces with drifilm and of coating Pyrex with SC-77.

It is believed that standard coating techniques with organosilane compounds such as SC-77 will leave OH sites on the coated surfaces [10]. Consider, for example, the process of coating Pyrex with SC-77. SC-77 is a mixture of $(\text{CH}_3)_2\text{SiCl}_2$ and $(\text{CH}_3)\text{SiCl}_3$. During the coating process, the SC-77 is combined with H_2O resulting in the Cl atoms being replaced by OH groups. The OH groups attached to the silane compounds will combine in such a way as to produce chains of Si-O bonds with methyl groups (CH_3) attached to the Si. These chains bond to the Pyrex surface to produce a surface of methyl groups. The methyl groups have a low dielectric constant and are fairly inert, therefore H or D atoms will tend not to stick to a surface of methyl groups. Consequently, these surfaces do not promote recombination of atoms to form molecules nor the spin relaxation of the polarized atoms. Occasionally, an OH group bonded to Si will remain in the final coating. As OH is a fairly polar and reactive molecule, the OH will be sites for relaxation and recombination of H or D atoms. Additionally, these sites will be subject to attack from K atoms, which are known to bond with OH.

To reduce the number of OH sites left in the final surface, a second coating, or afterwash, of a mixture containing trimethylmethoxysilane $((\text{CH}_3)_3\text{Si}(\text{COH}_3))$ is washed over the SC-77 coating. Ideally, the methoxy group (COH_3) will attach to the OH site to form a Si-O bond and the remaining surface will then contain only methyl groups. We obtain excellent results using this technique.

We use the atomic fraction as a measure of surface quality rather than the electron polarization because the atomic fraction samples all of the flow from the source, while measurements of the polarization select only the atoms in the flow, which in the event of significant molecular recombination on the surface is heavily weighted by the particles which experience the least collisions. Our experience is that f_a is a more sensitive monitor of the surface quality than P_e .

Fig. 2 shows f_a measurements made with the Pyrex glassware coated using the afterwash technique. The measurements were made without the storage cell in place, but the glassware and coating are the same as were used for

the p_{zz} measurements presented in section V. These do not represent "best ever" data, but represent the performance of the glassware used for the p_{zz} measurements. As seen in the figure, the atomic fraction is relatively stable for the three days data was taken. This is a marked improvement over f_a results for glassware coated with SC-77 alone which, in our experience, tends to yield a low f_a after being exposed to K for a similar amount of time.

Recently, the group at Argonne has been developing better coating techniques for Cu substrates. In the past, Cu substrates have been coated using a recipe similar to that used to coat aluminum substrates [10,1,11]. Both the work of Swenson and Anderson [11] and observations made at Argonne indicate that drifilm coatings on Cu rapidly deteriorate when exposed to alkali. We now have a new recipe for coating Cu substrates: The Cu substrate to be coated is cleaned with Alconox followed by washes of HCl and deionized water to both clean the surface and remove the oxide layer. This process is performed several times, finishing with the rinse of deionized water. Immediately following the cleaning procedure, the Cu piece is immersed in deionized water. To this is added equal amounts of dimethyldimethoxysilane and methyltrimethoxysilane, so that the final solution consists of 10% dimethyldimethoxysilane, 10% methyltrimethoxysilane, 80% deionized water,

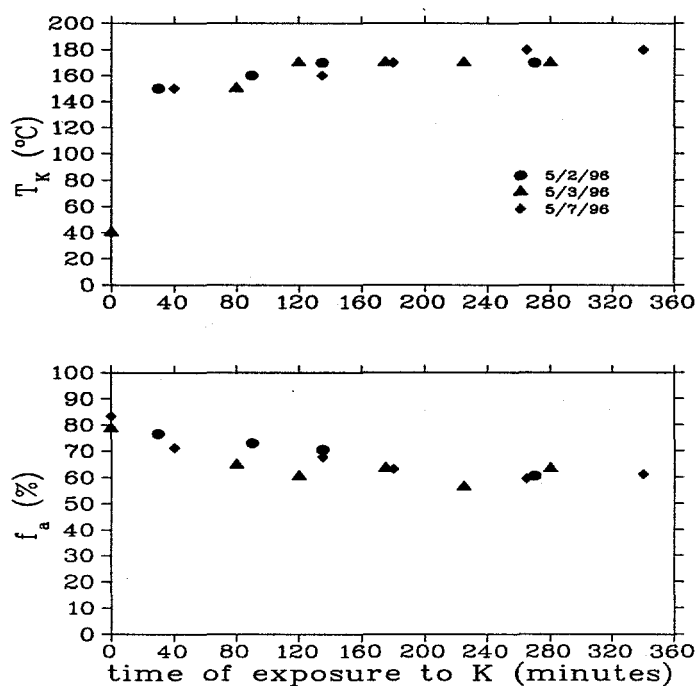


FIGURE 2. The atomic fraction f_a measured as a function of time exposed to K. The three symbols represent three different days of data. The upper graph shows the K ampule temperature as a function of the time corresponding to the f_a measurements, and thus is an indication of the K density in the optical pumping cell.

and enough HCl to raise the pH of the solution to between 2.7 and 3.1. The solution is not agitated. After 48 hours in the solution, the substrate is baked in vacuum for 24 hours at 225°C.

Researchers have found it difficult to consistently prepare SC-77 glass coatings which are clear and of some desired thickness. We have developed a method of coating glass with SC-77 which consistently yields a clear coating and allows one to control the coating thickness. The SC-77 coating procedure is performed in a hood filled with N₂. This prevents atmospheric water from reacting with the SC-77 before the coating is applied. The glass piece to be coated is suspended over a container holding 10 – 20 ml of SC-77. Deionized water is dripped into the container at a rate of about 0.02 ml/s. By steadily dripping the deionized water into the SC-77, the SC-77 is vaporized at a constant rate thus allowing one to control the amount of coating deposited on the surface. The glass piece is exposed to the SC-77 vapor for 2 to 20 minutes, depending on how thick a coating is desired, after which the glass piece is left in air for 30 to 60 minutes. An afterwash can then be performed or the piece can be directly baked in vacuum for 24 hours.

V POLARIZATION RESULTS

With the storage cell in place, both the electron polarization and nuclear tensor polarization can be measured as a function of flow. Fig. 3 shows P_e and p_{zz} measurements with $B = 600$ G in the optical pumping cell. The relative independence of P_e on flow is indicative that the system is in equilibrium over the entire range of flows investigated. Once n_D is great enough to achieve spin-temperature equilibrium, the dominant flow dependent mechanism for losing polarization is K-D spin-exchange collisions, which occur at a rate proportional to n_D . In this case, the 16% decrease in P_e should be reflected in a decrease in the alkali polarization P_K . This does not necessarily mean that P_K is a sensitive measurement of P_e , as a small change in P_K could result in a large change in P_e . Additionally, we have neglected other depolarization mechanisms that are dependent on D₂ density and hence flow, such as spin relaxation due to D – D₂ collisions and the loss of P_K due to K-D₂ collisions. To the authors knowledge, these spin relaxation rates have never been determined.

The helicity of the circularly polarized laser light was reversed to check for systematic effects. Other than the expected sign change, no dependence of $|P_e|$ or p_{zz} on laser light helicity can be seen within the error of the measurements. This is also a strong signature of spin-temperature equilibrium.

The measured p_{zz} is less than 0.035 for all the flows we tested. Assuming spin-temperature equilibrium, Eq. (1) can be used to calculate the electron polarization that one expects from the measured p_{zz} . The ratio of the electron polarization inferred from p_{zz} to that of the measured P_e is shown in Fig.

3(c). This ratio should be fairly free of experimental fluctuations such as laser frequency and power. The relative independence of this ratio with flow is a signature of spin-temperature equilibrium. On the average, the electron polarization inferred from spin-temperature, P_e^{ST} , is about 40% less than the measured P_e . This is not surprising since the electron polarimeter samples atoms from the transport tube, whereas the nuclear polarimeter samples along the length of the storage cell. Using Monte Carlo techniques, we estimate that the average D atom leaving the storage cell experiences about 650 more wall bounces than those detected in the P_e polarimeter. Therefore, we can use the formula $P_e^{ST} = P_e e^{-\frac{N}{N_{relax}}}$ to estimate the probability of relaxing per wall bounce, N_{relax}^{-1} . We calculate that $\langle N_{relax} \rangle = 1370$ wall bounces. It must be noted that the electron beam of the nuclear polarimeter ionizes atoms along the length of the storage cell, therefore 650 wall bounces represents an upper limit to the difference in wall bounces between the two polarimeters. $\langle N_{relax} \rangle$ could also be anomalously low due to poor coupling of the Pyrex transport tube to the aluminum tube, so that some of the atoms may interact with the viton O-ring or enter the O-ring groove. Therefore $\langle N_{relax} \rangle$ is not representative of wall conditions alone.

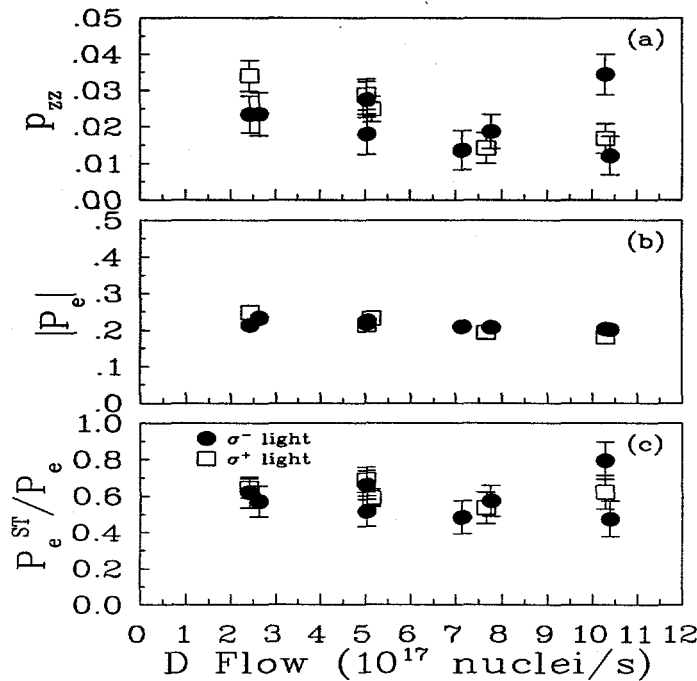


FIGURE 3. (a) p_{zz} vs. flow of D nuclei; (b) $|P_e|$ vs. flow of D nuclei; (c) the ratio of the electron polarization inferred from the p_{zz} data based upon spin-temperature equilibrium to the measured P_e as a function of D nuclei flow. All data is taken with of field of 600 G in the optical pumping cell.

VI CONCLUSION

In a laser-driven D target, wall relaxation is the dominant mechanism for loss of polarization and atomic fraction. We have developed new coating techniques which show improvements over previous methods used, both in terms of atomic fraction and the ability to obtain a consistent coating. We have also performed the first direct measurement of nuclear polarization in a laser-driven D target. This verifies that it is possible to obtain polarized deuterium nuclei without the use of rf transitions. The p_{zz} measurements provide further understanding of the operation of a laser driven target. A full report of the p_{zz} measurements is in preparation.

ACKNOWLEDGEMENTS

We are grateful to W. Haeberli, J. van den Brand, and the U. of Wisconsin for the loan of many parts of the nuclear polarimeter, and also to R. Holt and M. Poelker for their preliminary work on the polarimeter. We appreciate the skillful glassblowing of Joe Gregor, who made the laser-driven target glassware. This work is supported by the U.S. Department of Energy, Nuclear Physics Division, under contract No. W-31-109-ENG-38.

REFERENCES

1. J. A. Fedchak, C. E. Jones, and R. S. Kowalczyk, in *International Workshop on Polarized Beams and Polarized Gas Targets, Cologne, 1995* edited by H. P. gen. Schieck and L. Sydow (World Scientific, Singapore, 1996), pp. 72-79.
2. See M. Miller *et al.* in these proceedings.
3. Manuscript in preparation.
4. T. Walker and L. W. Anderson, *Nucl. Instrum. Methods A* **334**, 313 (1993).
5. M. Poelker *et al.*, *Phys. Rev. A* **50**, 2450 (1994).
6. M. Poelker *et al.*, *Nucl. Instrum. and Methods A* **364**, 58 (1995).
7. J. Stenger *et al.*, *Phys. Rev. Lett* **78**, 4177 (1997).
8. J. S. Price and W. Haeberli, *Nucl. Instr. Methods A* **326**, 416 (1993).
9. G. G. Ohlsen, J. L. McKibben, and G. P. Lawrence in *Polarization Phenomena in Nuclear Reactions, Proceedings of the Third International Symposium, Madison, 1970*, edited by H. H. Barschall and W. Haeberli (The University of Wisconsin Press, Madison, 1971), pp. 503-505.
10. J. A. Fedchak *et al.*, *Nucl. Instrum. Methods A* **XX**, xxx (1997).
11. D. R. Swenson and L. W. Anderson, *Nucl. Instrum. and Methods B* **12**, 157 (1985).